Supporting Information

CO_2 Methanation on Cu-cluster Decorated Zirconia Supports with Different Morphology: A Combined Experimental *in situ* GIXANES/GISAXS, *ex-situ* XPS and Theoretical DFT Study

Avik Halder[1€], Cristina Lenardi[2€], Janis Timoshenko[3€], Antonija Mravak[4€],

Bing Yang[1], Lakshmi K Kolipaka[1], Claudio Piazzoni[2], Sönke Seifert[5],

Vlasta Bonačić-Koutecký[4,6,7], Anatoly I. Frenkel,[3,8] Paolo Milani[2*], Stefan Vajda[1,9*]

[1] Materials Science Division, Argonne National Laboratory, 9700 South Cass Avenue, Lemont, IL 60439, United States

[2] C.I. Ma.I.Na., Dipartimento di Fisica, Università degli Studi di Milano, Via Celoria 16, I-20133 Milano, Italy

[3] Department of Materials Science and Chemical Engineering, Stony Brook University, Stony Brook, NY 11794 United States

[4] Center of Excellence for Science and Technology - Integration of Mediterranean region (STIM), Faculty of Science, University of Split, Ruđera Boškovića 33, CR-21000 Split, Croatia

[5] X-ray Science Division, Argonne National Laboratory, 9700 South Cass Avenue, Lemont, IL 60439, United States

[6] Interdisciplinary Center for Advanced Science and Technology (ICAST) at University of Split, Meštrovićevo šetalište 45, CR-21000 Split, Croatia

[7] Chemistry Department, Humboldt University of Berlin, Brook-Taylor-Straße 2, D-12489 Berlin, Germany

[8] Division of Chemistry, Brookhaven National Laboratory, Upton, NY 11973 United States

[9] Department of Nanocatalysis, J. Heyrovský Institute of Physical Chemistry, Czech Academy of Sciences, Dolejškova 3, CZ-18223 Prague 8, Czech Republic

[€] Equally contributing (first) authors

[*]Correspondence and requests for materials should be addressed to SV (stefan.vajda@jh-inst.cas.cz) or PM (Paolo.Milani@mi.infn.it)

Copper Cluster deposition.

Cu clusters were produced in a liquid nitrogen cooled magnetron sputtering source, the details for which can be found in Supplemental Information and in Ref.[1]. A brief overview of cluster production and deposition on the substrate is provided here.

Direct current (DC) argon sputtering of a 1 inch metal target at ~20 W power produces a cloud of metal vapor. Under a continuous flow 200 sccm of He and 200 sccm of Ar within the aggregation chamber maintained at a high pressure of several Torr, the copper vapor coalesces into Cu clusters of sizes ranging from a single atom to nanosized particles, both charged and neutral. The cationic Cu clusters exiting the aggregation chamber propagate down the beam path through a series of ion guides and finally a single cluster size is mass-selected using a quadrupole mass filter (9.5 mm Tri-Filter^{TM} from Extrel operating at 880 kHz). The clusters of specific size are then deposited onto zirconia supports. The mass spectrum of size-selected Cu clusters produced in the molecular beam is shown in Figure S2. The flux of charged clusters is monitored using a picoampermeter (Keithley Model 6489), and the amount of deposited material is determined from the integrated charge of clusters calculated during on line monitoring of the deposition current in real time by a custom LabVIEW program.[1] The deposition happened at a constant cluster ion current of 1 nA for Cu_4 and 300 pA for Cu_{12} clusters on ALD ZrOx support. On the thicker NS ZrOx support the ion current dropped gradually after the deposition started to ~ 40 – 50% of the maximum current at the beginning and then saturated at this lower value. This drop in deposition current on NS ZrOx, i.e., in the fraction of clusters being repelled from its charged surface, is due to slower charge dissipation on the thick oxide surface and neutralization of the charge by the compensation current from the picoampermeter measuring the deposition current in real time. The ALD ZrOx surface is very thin and thus the deposition process does not suffer from similar effects.

The deposition proceeds via a "soft-landing" technique where the impact energy of the clusters hitting the substrate is kept below 1 eV/atom. This prevents fragmentation of the clusters as previously confirmed from the TEM images taken for clusters deposited under similar.[2, 3] For this study, two 8 mm diameter cluster spots were deposited within which a surface coverage of 5% of an atomic monolayer (ML) equivalent was maintained. Such low coverage was chosen to maintain the size specificity of the catalyst when heated to high temperature.[2, 4, 5] The total copper loading per cluster spot in these samples is about 5 nanograms (4.45×10^{13} atoms).[1]

In situ GIXANES, GISAXS, and TPRx.

The testing of performance and characterization of the working catalyst was performed in a home-built reactor at beamline 12-ID-C of the Advanced Photon Source at the Argonne National Laboratory.[6] This experimental setup allows *in situ* X-ray monitoring of changes in the size of the clusters and follow the changes in the oxidation state of the metal, as well as to simultaneously monitor reaction product formation during temperature programmed reaction (TPRx). The details for the reactor have and the *in situ* experimental setup have been reported elsewhere.[6, 7] Reaction products were analyzed on a quadrupole mass spectrometer (Pfeiffer Prisma QMS 200) sampling the reaction mixtures through an electronic valve (EVR 116, Pfeiffer) on the inlet of the mass which, in a feedback loop with a pressure gauge allows to keep a constant pressure (5×10^{-6} mbar) in the mass spectrometer. The reactor was maintained at a pressure of 1.1 atm with a continuous 18 sccm flow of pure CO_2 and H_2 in 1:3 ratio. We also detected the presence of ~ 100 ppm of residual O_2 in the reaction mixture. The reaction was performed using a uniform double heat and cool ramp (Figure 1a), in order to identify potential changes in the catalytic performance with time should the catalyst change during the heating and cooling cycles. Furthermore, the symmetric heating-cooling ramp was repeated twice with a 90 minutes cool down in between to check the reproducibility in the catalytic performance as shown in. For the on-line analysis of the gas mixture exiting from the reaction cell during the course of the reaction, we used our mass spectrometer put in multi-ion-detection mode (MID). This operation mode allows for a simultaneous monitoring of the ion current corresponding to the characteristic mass peaks of products. The mass spectrometer was calibrated using gases diluted in helium purchased from AirGas; three concentrations were used (including 100% He) by further mixing with pure helium in a gas mixer manifold equipped with precision mass flow controllers (Brooks), to ensure linearity. The reaction rate of methane formation (r_{CH4}) is calculated, defined as the number of methane molecules formed per total Cu atom per second (in units of molecules $atom^{-1}$ sec^{-1}). The uncertainty in the mass spectrometer signal has been estimated from standard deviation of 23 data points collected during the last 5 minutes at each temperature plateau following equilibration of the ion current. The uncertainty is plotted in the plot of r_{CH4} in Figure 1 (b-e).

In order to probe the changes in the oxidation state of copper in the cluster under reaction conditions, we collected X-ray absorption near-edge spectra at a grazing incidence (GIXANES). To maximize the sensitivity of the experiment to the clusters lying on the surface of the support, the X-ray beam was scattered off the sample surface close to the angle of total reflection, i.e., the critical grazing incident angle of 0.3°. An additional advantage of the low angle is that a long stripe of the sample surface is illuminated, which significantly increases measured signal levels in the case of samples with very low metal coverage. GIXANES data were collected at Cu K edge (8.9 keV) by a 4-element fluorescence detector (Vortex) mounted parallel to the sample surface in order to minimize background from elastic scattering. The spectra of the Cu metal foil, Cu_2O, CuO, and $Cu(OH)_2$ bulk standards were collected at the 12-BM beamline of the Advanced Photon Source in transmission mode (shown in Figure 2a). These spectra were used as reference spectra for linear combination fit (LCF) analysis of the XANES spectra.

Note here that the local structure in ultra-small clusters deviate from that in the bulk standards. Therefore in this work we complement the LCF approach by an multivariate curve resolution with alternating least-squared (MCR-ALS) method,[8] which has proven to be instrumental for speciation of mixtures, when the exact reference spectra for pure components are not known.

A complementary small-angle X-ray scattering measurement was performed at grazing incidence (GISAXS), to monitor possible agglomeration Cu clusters during the reaction.[6, 9, 10] The X-ray beam of 9.1 keV energy was scattered off the sample at the angle of incidence, 0.15˚ (chosen near the critical angle of 0.18˚ of the silicon substrate), and the two-dimensional GISAXS images were

collected on a 1024 × 1024 pixel two – dimensional Gold (modular CCD area) detector.[11] The 2D X-ray images were taken from the cluster sample at each value of temperature of the temperature ramp. The 2D scattering pattern were analyzed to obtain information about changes in the lateral and vertical dimensions of the particles, by taking cuts in the horizontal and vertical direction of the GISAXS image [11] and analyzing of these cuts with the Modelling II tool in the Irena tool suite.[12]

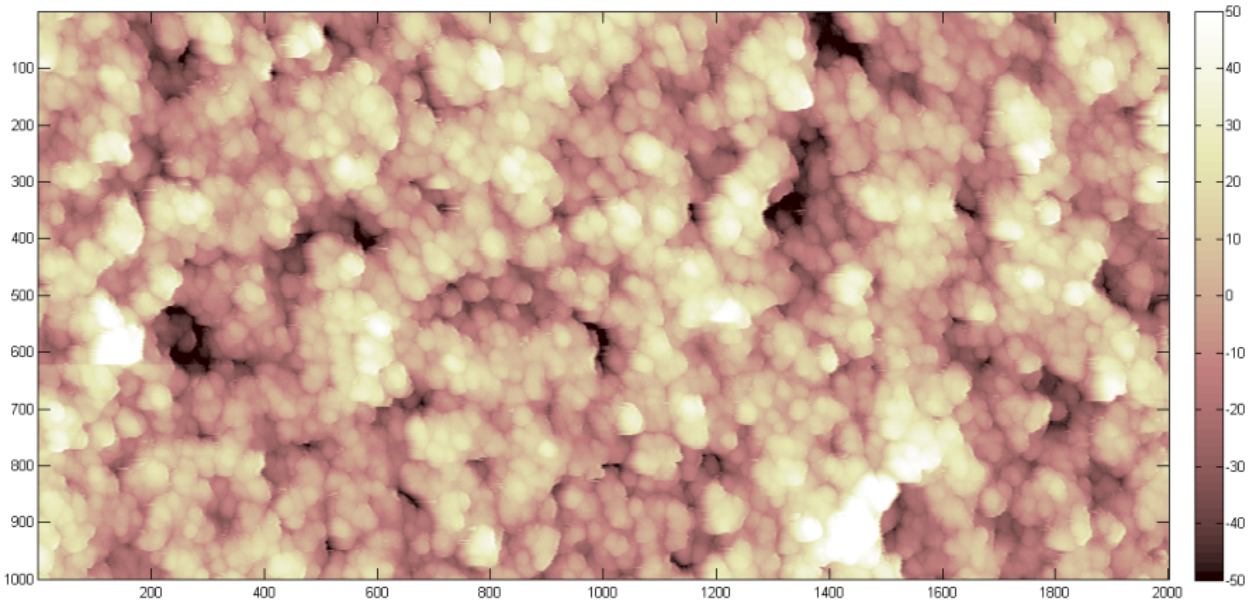

Figure S1. AFM image of the NS-ZrOx film (2x1x0.1µm), Coating thickness from stylus profilometry on side of the silicon wafer: 125nm, roughness 18.5 ± 0.4 nm, specific surface area 300 m^2/g

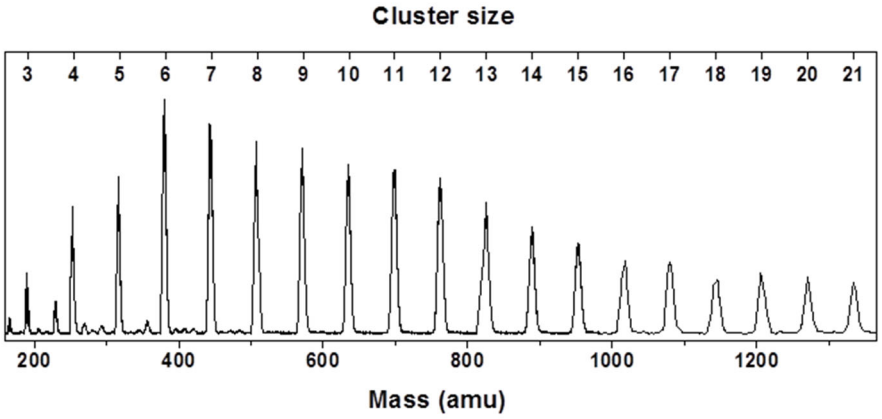

Figure S2. Mass spectrum of copper positively charged copper clusters, showing mass (amu) on the bottom x-axis and corresponding nuclearity on the top axis.

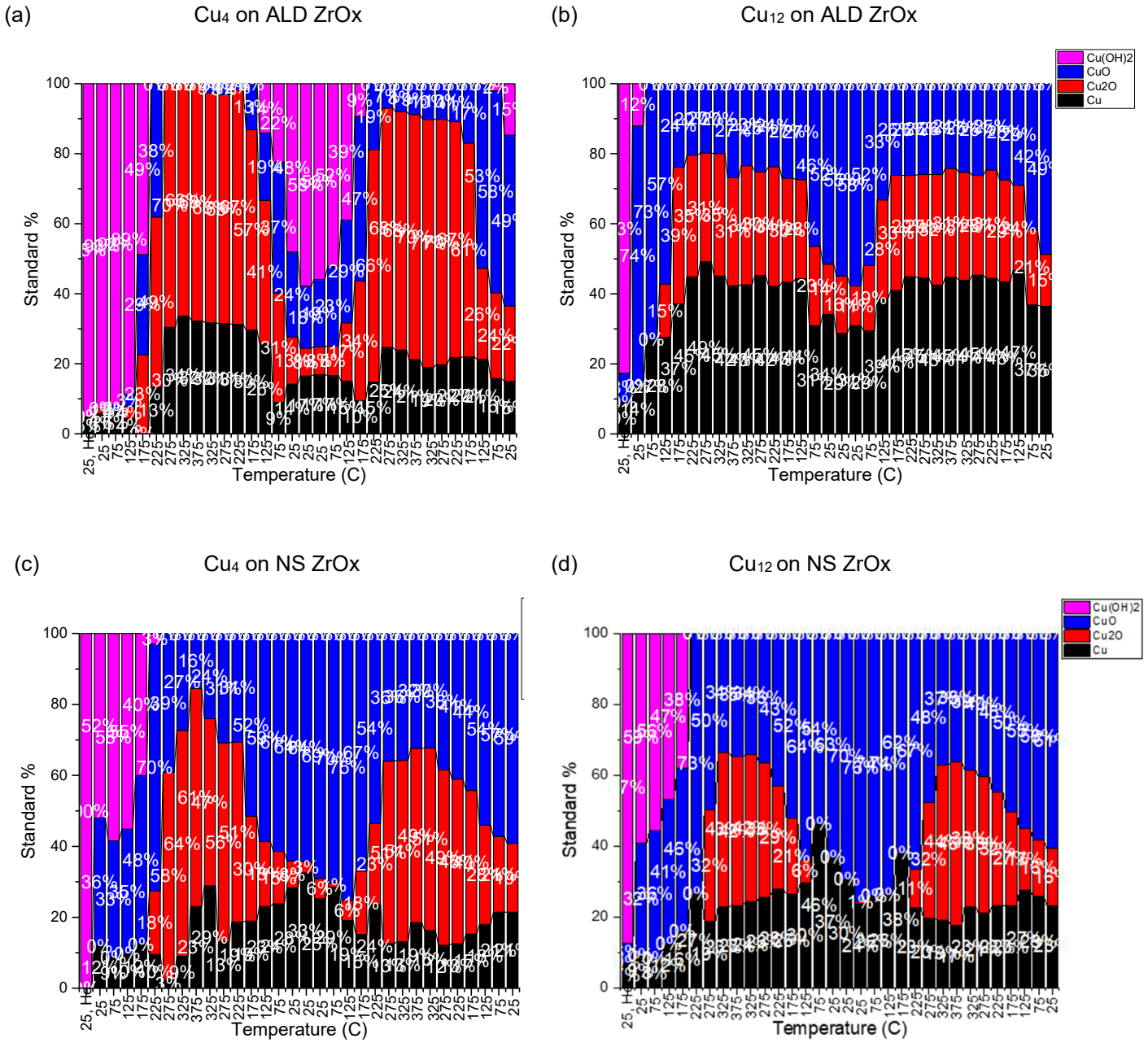

Figure S3: Change in composition of clusters during the heat ramp from Figure1a. (a) Cu_4 on ALD ZrOx; (b) Cu_{12} on ALD ZrOx; (c) Cu_4 on NS ZrOx; (d) Cu_{12} on NS ZrOx.

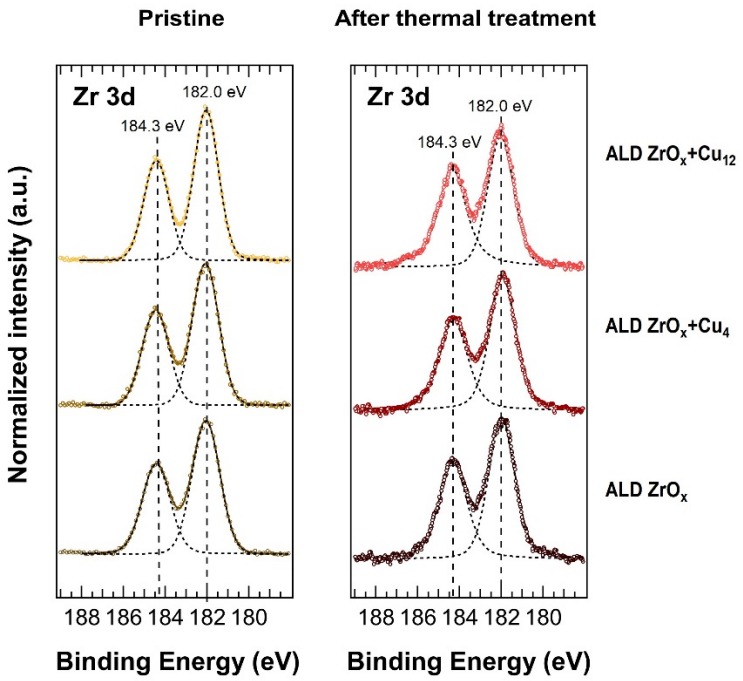

Figure S4: Fitted normalized Zr 3d spectra of pristine and after the complete thermal process for ALD ZrO_x samples.

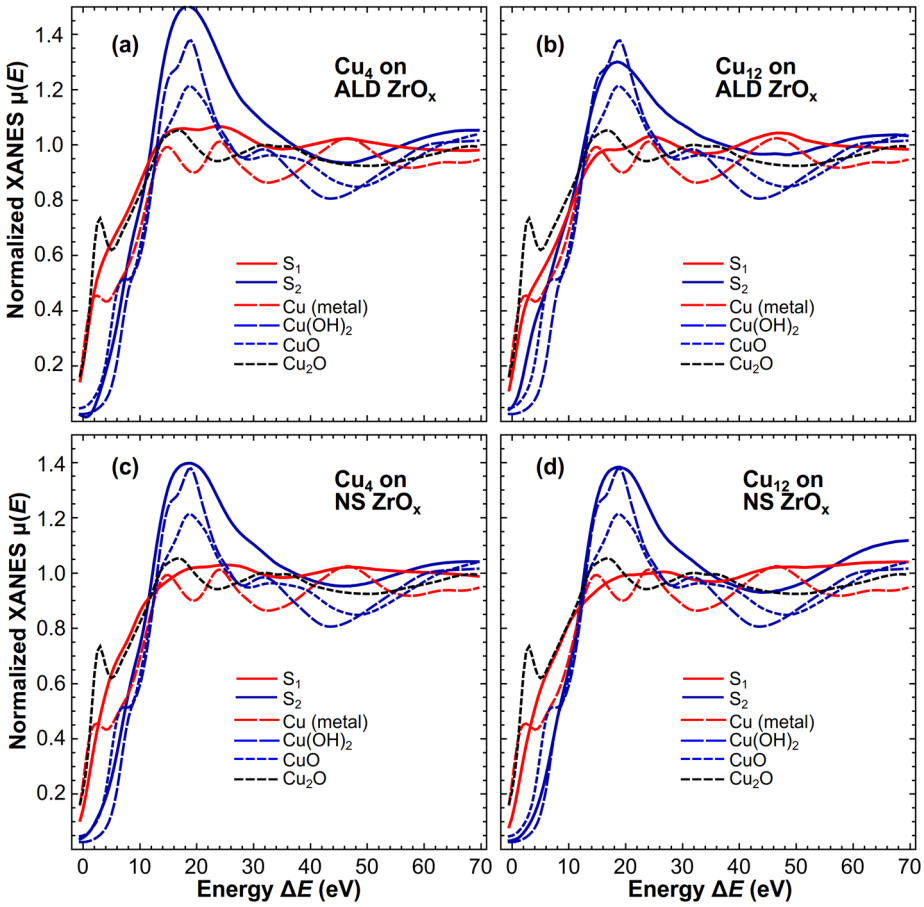

Figure S5. Spectra of pure compounds as obtained from MCR-ALS analysis for Cu_4 on ALD ZrOx (a), Cu_{12} on ALD ZrOx (b), Cu_4 on NS ZrOx (c) and Cu_{12} on NS ZrOx (d). XANES spectra S_1 and S_2 for two species identified by MCR-ALS method are shown as solid lines and compared with experimental spectra for bulk reference materials (metallic Cu, Cu_2O, CuO and $Cu(OH)_2$, dashed lines). Temperature-dependencies of the weights of contribution of S_2 (which resembles spectrum for oxide) to the total spectra are shown in Figure 5 in the main text.

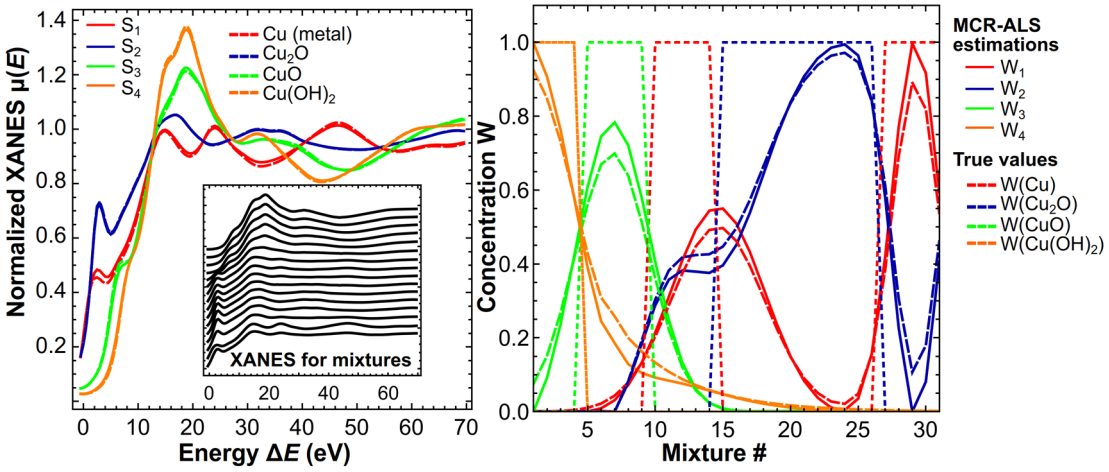

Figure S6. Validation of MCR-ALS method with model data**.** 31 XANES spectra (left panel, inset) for mixtures of metallic Cu, Cu^{+} and Cu^{2+} species were modeled as linear combinations of experimental Cu K-edge EXAFS spectra for metallic Cu, Cu_2O, CuO and $Cu(OH)_2$ (left panel, dashed lines). Employed concentration profiles are shown in the right panel (dashed lines). MCR-ALS method was then applied to reconstruct the concentration profiles and original spectra from XANES spectra for mixtures. Initial concentration profiles, used as input for MCR-ALS method, are shown as dotted lines in the right panel. Final concentration profiles W_1, W_2, W_3 and W_4, reconstructed by MCR-ALS method for identified four species, are shown as solid lines in the right panel. Corresponding XANES spectra S_1, S_2, S_3 and $S_4$for four identified species are shown as solid lines in the left panel. Spectra are in an excellent agreement with the original spectra, used to construct spectra for mixtures, while the reconstructed concentration profiles agree well with the true profiles, used to construct model spectra.

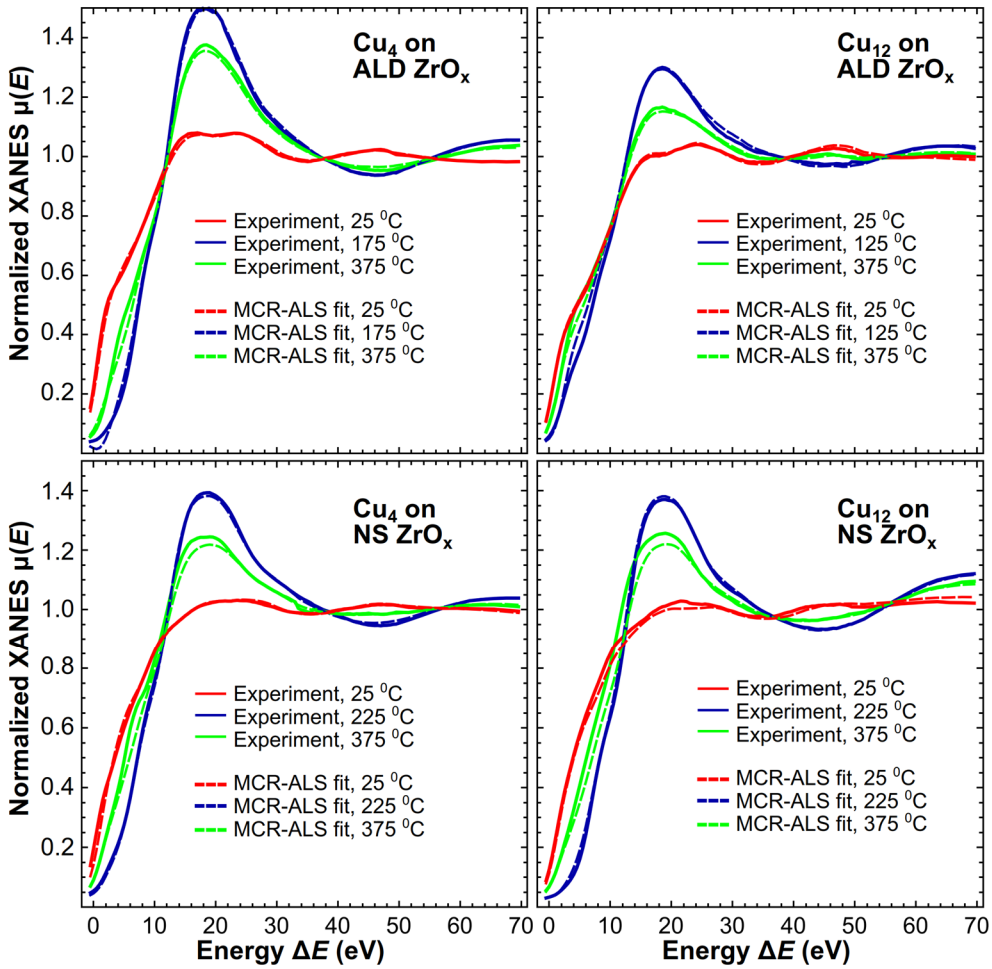

Figure S7. Typical fits of experimental data with MCR-ALS method. Experimental XANES spectra for Cu_4 and Cu_{12} clusters on ALD and NS ZrOx, obtained at 25^0C, 375^0C and at intermediate temperature (first heating cycle) are shown as solid lines. Corresponding MCR-ALS fits are shown with dashed lines.

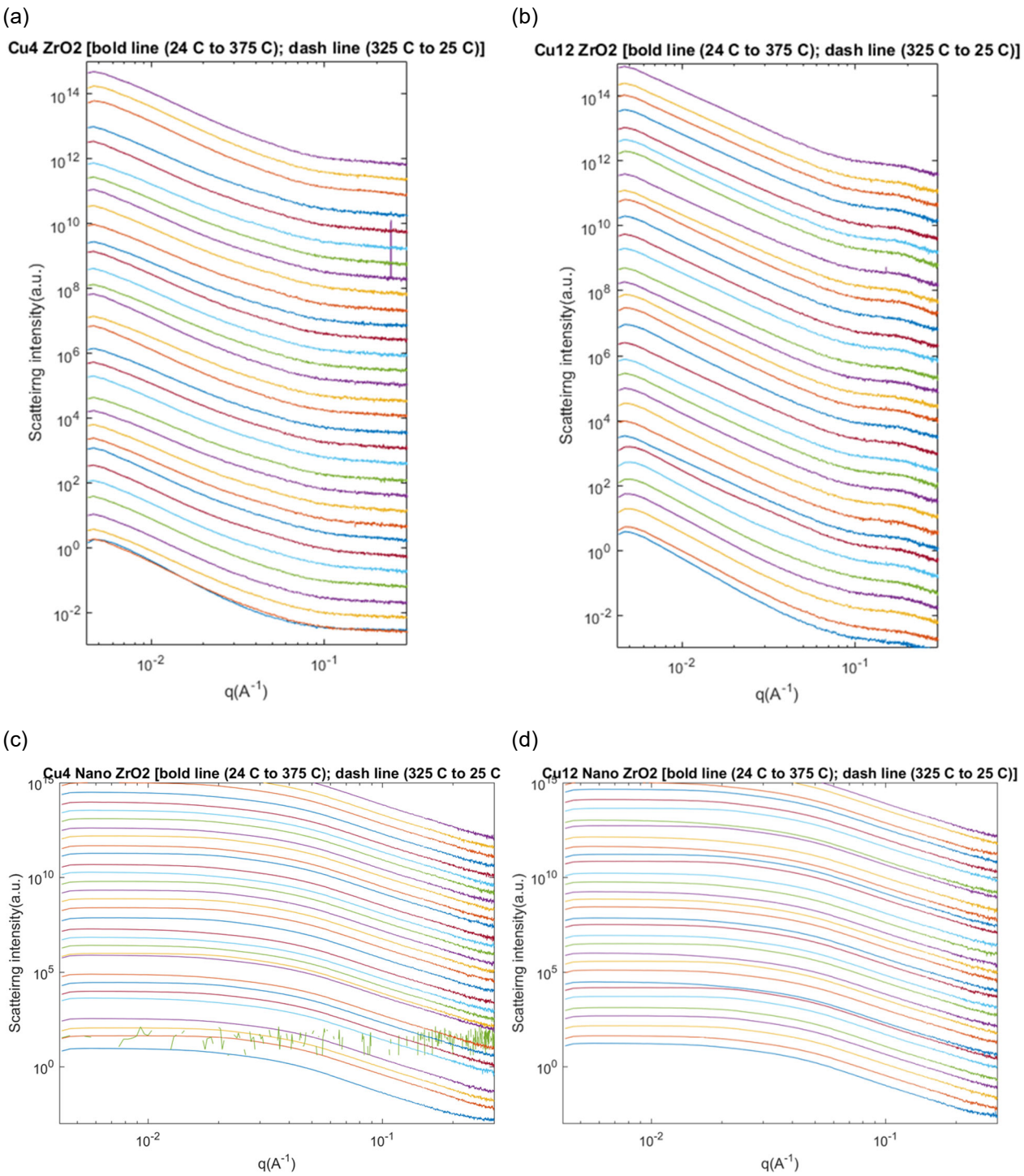

Figure S8. Horizontal GISAXS cuts. (a) Cu_4 on ALD ZrOx; (b) Cu_{12} on ALD ZrOx; (a) Cu_4 on NS ZrOx; (b) Cu_{12} on NS ZrOx.

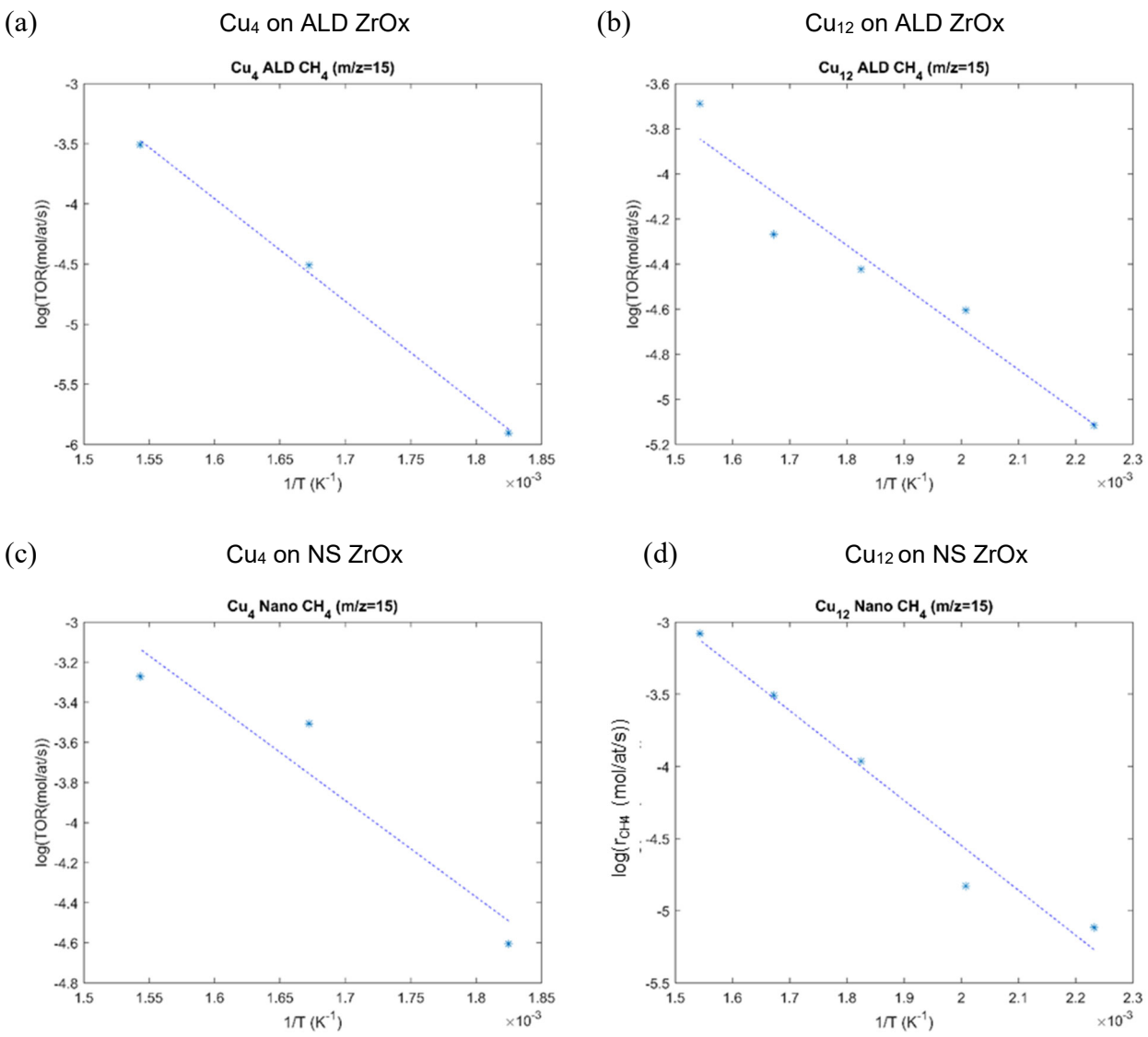

Figure S9. Arrhenius plot for activation energy (Ea) calculation. (a) Cu_4 on ALD ZrOx; (b) Cu_{12} on ALD ZrOx; (a) Cu_4 on NS ZrOx; (b) Cu12 on NS ZrOx.

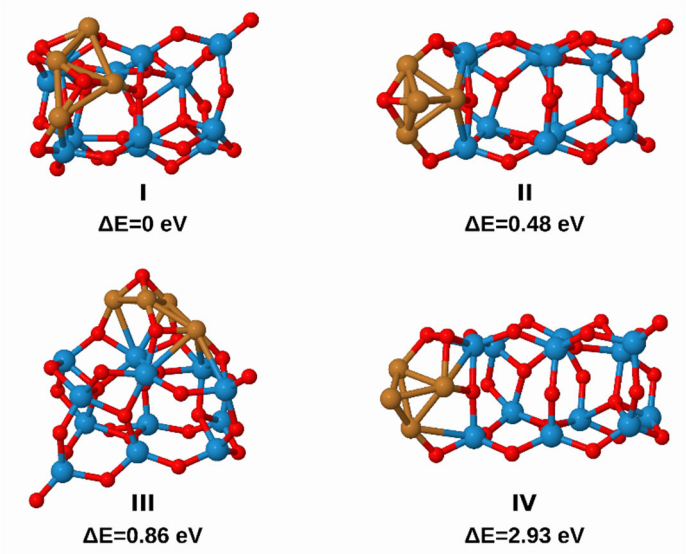

Figure S10. Isomers of $Cu_4O_2Zr_{12}O_{24}$ obtained by DFT using B3LYP functional, def2-SV(P) basis and relativistic effective core potential RECP for Zr atoms, illustrating energetically favorable isomer I containing Cu_4 rhombic structure interacting with Zr and O atoms of $Zr_{12}O_{24}$.

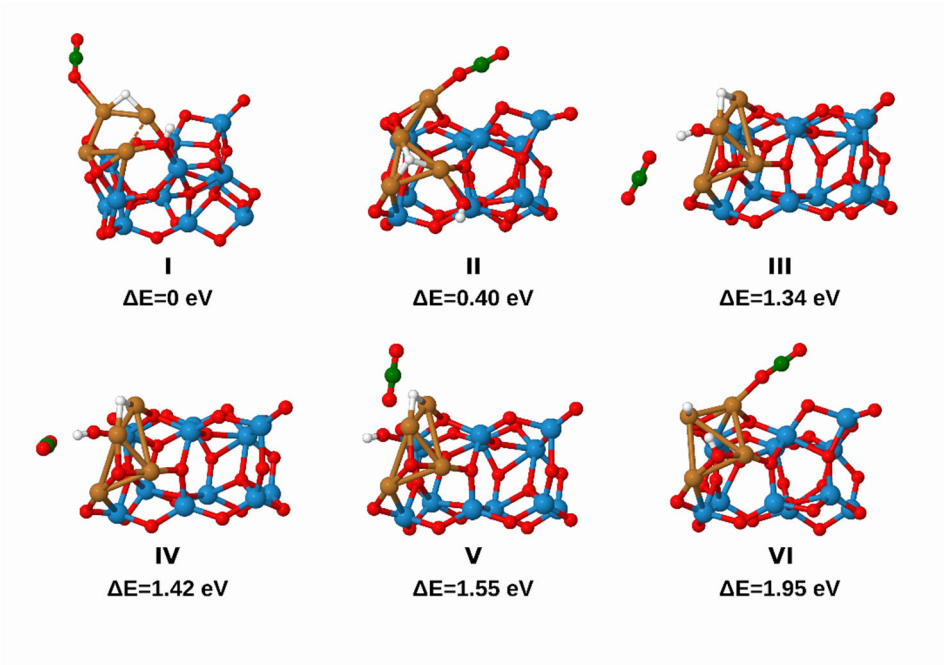

Figure S11. Isomers of $CO_2H_2Cu_4O_2Zr_{12}O_{24}$. The lowest energy isomer I serves as a starting point for methanation reaction and involves CO_2 bound to one of copper atoms of Cu_4O_2 subunit, which is connected with the support. One of the hydrogen atoms is bound to 2 copper atoms and the other one to the oxygen of the support playing the role in hydrogenation steps. B3LYP functional, def2-SV(P) basis set and relativistic effective core potential RECP for Zr atoms have been used within DFT method.

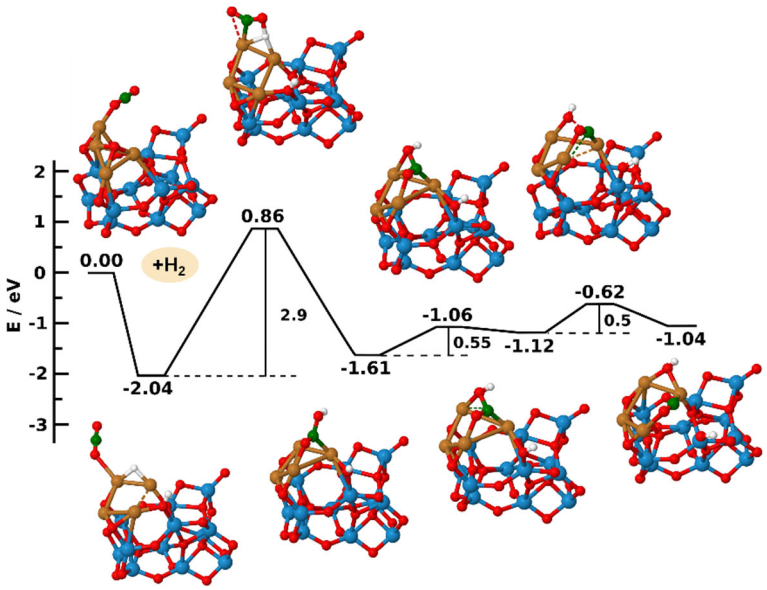

Figure S12. Calculated energy profile of reaction pathway of CO_2 on oxidized copper tetramer (Cu_4O_2) supported by $Zr_{12}O_{24}$ following hydrogenation step over formation of COOH dissociated into CO and OH, using B3LYP functional, def2-TZVP basis set and relativistic effective core potential RECP for Zr atoms within DFT method.

References – Supporting Information

1. Yin, C.; Tyo, E.; Kuchta, K.; Issendorff, B. v.; Vajda, S., Atomically precise (catalytic) particles synthesized by a novel cluster deposition instrument. *J Chem. Phys.* **2014,** *140* (17), 174201.
2. Timoshenko, J.; Halder, A.; Yang, B.; Seifert, S.; Pellin, M. J.; Vajda, S.; Frenkel, A. I., Subnanometer Substructures in Nanoassemblies Formed from Clusters under a Reactive Atmosphere Revealed Using Machine Learning. *J Phys. Chem. C* **2018,** *122* (37), 21686-21693.
3. Lu, J.; Cheng, L.; Lau, K. C.; Tyo, E.; Luo, X.; Wen, J.; Miller, D.; Assary, R. S.; Wang, H.-H.; Redfern, P.; Wu, H.; Park, J.-B.; Sun, Y.-K.; Vajda, S.; Amine, K.; Curtiss, L. A., Effect of the size-selective silver clusters on lithium peroxide morphology in lithium–oxygen batteries. *Nat Commun* **2014,** *5*, 4895.
4. Negreiros, F. R.; Halder, A.; Yin, C.; Singh, A.; Barcaro, G. ; Sementa, L.; Tyo, E. C.; Pellin, M. J.; Bartling, S.; Meiwes-Broer, K.-H.; Seifert, S.; Sen, P.; Nigam, S.; Majumder, C.; Fukui, N. H. ; Yasumatsu, ; Vajda, S. and ; Fortunelli A., Bimetallic Ag-Pt Sub-nanometer Supported Clusters as Highly Efficient and Robust Oxidation Catalysts. *Angew. Chem. Int. Ed.* **2018,** *57* (5), 1209-1213.
5. Tyo, E. C.; Vajda, S., Catalysis by clusters with precise numbers of atoms. *Nat. Nanotechnol.* **2015,** *10*, 577.
6. Lee, S.; Lee, B.; Seifert, S.; Vajda, S.; Winans, R. E., Simultaneous measurement of X-ray small angle scattering, absorption and reactivity: A continuous flow catalysis reactor. *Nuclear Instruments and Methods in Physics Research Section A: Accelerators, Spectrometers, Detectors and Associated Equipment* **2011,** *649* (1), 200-203.
7. Lei, Y.; Mehmood, F.; Lee, S.; Greeley, J.; Lee, B.; Seifert, S.; Winans, R. E.; Elam, J. W.; Meyer, R. J.; Redfern, P. C.; Teschner, D.; Schlögl, R.; Pellin, M. J.; Curtiss, L. A.; Vajda, S., Increased Silver Activity for Direct Propylene Epoxidation via Subnanometer Size Effects. *Science* **2010,** *328* (5975), 224-228.
8. Martini, A.; Borfecchia, E., Spectral Decomposition of X-ray Absorption Spectroscopy Datasets: Methods and Applications. *Crystals* **2020,** *10* (8), 664.
9. Lee, B.; Seifert, S.; Riley, S. J.; Tikhonov, G.; Tomczyk, N. A.; Vajda, S.; Winans, R. E., Anomalous grazing incidence small-angle x-ray scattering studies of platinum nanoparticles formed by cluster deposition. *J Chem. Phys.* **2005,** *123* (7), 074701.
10. Keshari, A. K.; Pandey, A. C., Size and Distribution: A Comparison of XRD, SAXS and SANS Study of II–VI Semiconductor Nanocrystals. *J. Nanosci. Nanotechnol.* **2008,** *8* (3), 1221-1227.
11. Wyrzgol, S. A.; Schafer, S.; Lee, S.; Lee, B.; Vece, M. D.; Li, X.; Seifert, S.; Winans, R. E.; Stutzmann, M.; Lercher, J. A.; Vajda, S., Combined TPRx, in situ GISAXS and GIXAS studies of model semiconductor-supported platinum catalysts in the hydrogenation of ethene. *Phys. Chem. Chem. Phys.* **2010,** *12* (21), 5585-5595.
12. Jan, I.; R., J. P., Irena: tool suite for modeling and analysis of small-angle scattering. *J. Appl. Cryst.* **2009,** *42* (2), 347-353.